Yokota O, Tsuchiya K, Itoh Yoshinori, Ishizu H, Akiyama H, Ikeda M, Kuzuhara S, Otomo E	Frontotemporal lobar degeneration with ubiquitin pathology: an autopsy case presenting with semantic dementia and upper motor neuron signs with a clinical course of 19 years	Acta Neuropathol	112	739-749	2006
Matsumoto N, Ikeda M, Fukuhara R, Shinagawa S, Ishikawa T, Mori T, Toyota Y, Matsumoto T, Adachi H, Hirono N, Tanabe H	Caregiver's burden associated with behavioral and psychological symptoms of dementia in the local community elderly people	Dement Geriatr Cogn Disord			in press
Toyota Y, Ikeda M, Shinagawa S, Matsumoto T, Matsumoto N, Hokoishi K, Fukuhara R, Ishikawa T, Mori T, Adachi H, Komori K, Tanabe H	Comparison of behavioral and psychological symptoms in early-onset and late-onset Alzheimer's disease	Int J Geriatr Psychiatry			in press
松本伊津美，小森憲治郎，池田　学，田辺敬貴	高齢発症の意味認知症の一例	愛媛十全医療学院紀要	6	23-26	2006
松本直美，池田　学，福原竜治，兵頭隆幸，石川智久，森　崇明，豊田泰孝，松本光央，足立浩祥，品川俊一郎，鉾石和彦，田辺敬貴，博野信次	日本語版 NPI-D と NPI-Q の妥当性と信頼性の検討	脳神経	58	785-790	2006
松本光央，池田　学，豊田泰孝，石川智久，上村直人，博野信次，田辺敬貴	アルツハイマー病の運転能力低下に関するスクリーニング検査ードライビングシミュレーターを用いた運転能力評価についてー	老年精神医学雑誌	17	977-985	2006
安部幸志，荒井由美子，福原竜治，池田学	家族が認知症となった場合の対処行動ー一般生活者に対する調査からー	日本医事新報	4292	63-67	2006
池田　学	痴呆の精神症状と行動異常ーグループホームにおける課題ー	臨床精神薬理	9	1106-1112	2006
池田　学	前頭側頭型痴呆の臨床	Dementia Japan	19	17-26	2006
池田　学	内科医のための脳疾患講座　前頭側頭型痴呆（認知症）その 2	BRAIN MEDICAL	18	98-102	2006
松本伊津美，小森憲治郎，松本直美，池田　学	語彙の脳内機構と Semantic Dementia	CLINICAL NEUROSCIENCE	24	547-550	2006

小森憲治郎, 石丸三和子, 池田　学, 田辺敬貴	緩徐進行性失語	CLINICAL NEUROSCIENCE	24	777-780	2006
池田　学	前頭側頭型認知症の臨床と画像診断	Mebio	23	57-63	2006
Ikeda M	Interventional studies with the aim of reducing the burden of care through drug therapy of BPSD	Acta Neurologica Taiwanica	15	65-66	2006
福原竜治, 鉾石和彦, 蓮井康弘, 池田　学	認知症を地域で支える　大学病院の役割	老年精神医学雑誌	17	503-509	2006
上村直人, 池田　学, 荒井由美子, 野村美千江, 博野信次	認知症と社会的側面　わが国における認知症ドライバー研究の動向	脳神経	58	463-470	2006
品川俊一郎, 足立浩祥, 池田　学	最初期の認知障害	Pharma Medica	24	35-38	2006
森　崇明, 池田　学	BPSD に対する薬物療法	精神科	9	43-47	2006
池田　学, 上村直人, 荒井由美子, 野村美千江, 博野信次	認知症高齢者の自動車運転と権利擁護に関する研究	公衆衛生	70	692-694	2006
上村直人, 池田　学	認知症と自動車運転ー医療からみたわが国における現状と課題ー	実践成年後見	19	93-101	2006
池田　学	BPSD に対する非定型抗精神病薬の使用をめぐって	精神医学	48	1165-1167	2006
繁信和恵, 池田　学	前頭側頭型認知症の初期診断	モダンフィジシャン	26	1865-1871	2006
石川智久, 池田　学, 田辺敬貴	愛媛県中山町研究の結果から明らかになってきた課題	老年精神医学雑誌	17 増刊号 II	61-66	2006
池田　学	中山町研究ー地域での痴呆（認知症）予防を目指してー	第 11 回脳循環 SPECT・PET カンファレンス抄録集		13-18	2006
池田　学	巻頭言　日本の認知症臨床のレベルと今後に期待すること	老年精神医学雑誌	18	6-7	2007

樫林哲雄，石川智久，田辺敬貴，秦　龍二，池田　学	MCI と LNTD	分子精神医学	27		印刷中
池田　学	FTLD 等認知症周辺症状のマネージメント	分子精神医学	27		印刷中
石井賢二	アルツハイマー病の早期診断に有効なのはアミロイドイメージングか、脳代謝・血流画像か　アミロイドイメージングであるとの立場から.	Cognition and Dementia	6(1)	68-73	2007
Kimura Y, Naganawa M, Yamaguchi J, Uchiyama A, Oda K, Ishii K, Ishiwata K	MAP-based Kinetic Analysis for Voxel-by-Voxel Compartment Model Estimation: Detailed Imaging of the Cerebral Glucose Metabolism using FDG.	NeuroImage	29(4)	1203-1211	2006
Itokawa K, Tamura N, Kawai N, Shimazu K, Ishii K	Parkinsonism in Type I Gaucher's Disease.	Internal Medicine	45(20)	1165-1167	2006
Saito Y, Ishii K, Yagi K, and H Mizusawa.	Cerebral networks for spontaneous and synchronized singing and speaking.	NeuroReport	17(18)	1893-1897	2006
Ishiwata, K., Oda, K., Sakata, M., Kimura, Y., Kawamura, K., Oda, K., Sasaki, T., Naganawa, M., Chihara, K., Okubo, Y., Ishii, K.	A feasibility study of [11C]SA4503-PET for evaluating sigma1 receptor occupancy by neuroleptics: the binding of haloperidol to sigma1 and dopamine D2-like receptors.	Ann Nucl Med	20(10)	569-573	2006
藤原佳典、西真理子、渡辺直紀、李相侖、井上かず子、吉田裕人、佐久間尚子、呉田陽一、石井賢二、内田勇人、角野文彦、新開省二.	都市部高齢者による世代間交流型ヘルスプロモーションプログラム　"REPRINTS"の1年間の歩みと短期的効果.	日本公衆衛生学会誌	53(9)	702-714	2006
石井賢二.	脳疾患における PET の現状と展望.	映像情報 Medical	38(11)	1044-1053	2006
石井賢二.	動的神経病理としての PET.	臨床検査	50(10)	1099-1105	2006
Gerloff C, Bushara K, Sailer A, Wassermann EM, Chen R, Matsuoka T, Waldvogel D, Wittenberg GF, う, Cohen LG, and Hallett M.	Multimodal imaging of brain reorganization in motor areas of the contralesional hemisphere of well recovered patients after capsular stroke.	Brain	129(3)	791-808	2006

Tanaka Y, Nariai T, Nagaoka T, Akimoto H, Ishiwata K, Ishii K, Matsushima Y and Ohno K.	Quantitative evaluation of cerebral hemodynamics in patients with moyamoya disease by dynamic susceptibility contrast magnetic resonance imaging. - Comparison with positron emission tomography-.	J Cereb Bllod Flow Metab	26(2)	291-311	2006
小山恵子	もの忘れ：外来診療と鑑別診断の流れ	性差と医療	3(11)	1129-1134	2006
須田潔子、小山恵子	アルツハイマー病の診断と治療	性差と医療	3(11)	1139-1142	2006
Matsuda H	Functional neuroimaging in Alzheimer's disease.	Radiation medicine	24(4)	302-308	2006
Kawachi T, Ishii K, Sakamoto S, Sasaki M, Mori T, Yamashita F, Matsuda H, Mori E	Comparison of the diagnostic performance of FDG-PET and VBM-MRI in very mild Alzheimer's disease.	Eur J Nucl Med Mol Imaging	33(7)	801-809	2006
Nakano S, Asada T, Yamashita F, Kitamura N, Matsuda H, Hirai S, Yamada T	Relationship between antisocial behavior and regional cerebral blood flow in frontotemporal dementia.	Neuroimage	32(1)	301-306	2006
Kuroda R, Satoh J, Yananura T, Anezaki T, Terada T, Yamazaki K, Obi T, Mizoguchi K	A novel compound heterozygous mutation in the DAP12 gene in a patient with Nasu-Hakola disease	Journal of the Neurological Science	252	88-91	2007
小尾智一	Familial PD	臨床検査	50	1165-1170	2006
Takao M, Tsuchiya K, Mimura M, Momoshima S, Kondo H, Akiyama H, Suzuki N, Mihara B, Takagi Y, KotoA.	Corticobasal degeneration as cause of progressive non-fluent aphasia: a clinical, radiological and pathological study of an autopsy case.	Neuropathology	26	569–578	2006
Takao M, Akiyama H, Kaburagi H, Ogata K.	Familial spastic paraplegia of two siblings – clinical and neuropathologic analysis	Brain Pathol	16	S64	2006
Takao M, Sato H, Suzuki N, Nishino I, Yoshikawa T, Ishihara T.	A case report of possible myotonic dystrophy without DM1 OR DM2 gene mutations. Clinical and pathologic a	Brain Pathol	16	S145	2006

	nalyses.				
Sato H, Takao M, Suzuki N, Araha ta H, Nishino I, Yoshikawa T, Isihara D.	A case report of myopathy with unusual clinical and pathologic presen tation.	Neuropathology	26	A49	2006
美原淑子, 高畑君子, 栗原真弓, 高橋陽子, 永島隆秀, 冨田裕, 高尾昌樹, 美原盤.	音楽療法によりQuality of Lifeが向上した筋萎縮性側索硬化症患者の1例 Schedule for the Evaluation of Individual Quali ty of Life-Direct Weightingによる評価.	日本音楽療法学会誌	6	33-40	2006
美原盤, 美原淑子, 藤本幹雄, 永島隆秀, 冨田裕, 高尾昌樹.	筋萎縮性側索硬化症に対する音楽療法 神経心理学的検査と生理学的側面からの検討.	日本音楽療法学会誌	6	23-32	2006
高尾昌樹, Ghetti B	【認知症の動的神経病理】 アルファシヌクレイノパチー	臨床検査	50	1130-1136	2006
高尾昌樹	Presenilin 1の新規S170F変異を伴う, 20代発症のLewy小体を伴う家族性アルツハイマー病	Brain & Nerve	15	5	2006
高尾昌樹, 厚東篤生	ラクナ梗塞の病理	日本臨床	64(増8)	134-138	2006
秋山久尚, 百島祐貴, 高尾昌樹, 荒崎圭介, 星野晴彦	左片麻痺で発症し,多彩な頭部画像変化を認めた39歳男性剖検例	脳と神経	58	347-362	2006
高尾昌樹, 厚東篤生	スポーツ医学エビデンス 身体活動で疾病は予防・改善可能か? 脳血管疾患	臨床スポーツ医学	23	693-700	2006
高尾昌樹	こむら返り	神経内科	64	334-340	2006
高尾昌樹	素顔のニューロサイエンティスト	Clinical Neuroscience	25	117	2007

研究成果の刊行に関する一覧表
(2006年4月1日ー2007年3月31日迄)

書籍

編著者氏名	論文タイトル名	書籍全体の編集者名	書　籍　名	出版社名	出版地	出版年	ページ
村山繁雄	軽度認知障害の背景病理解明のためのクリニカルパス	村山繁雄	アルツハイマー病診断 - 早期発見・早期介入のために	真興出版	東京	2006.1	15-18
村山繁雄・齊藤祐子	PDD（認知症を伴うパーキンソン病）とDLB（レヴィー小体型認知症）の臨床と病理		Annual Review 神経 2007	中外医学社	東京	2007	167-174
石井賢二	アルツハイマー病診断：画像（PET）	村山繁雄	アルツハイマー病診断	真興交易出版	東京	2006.7	15-18
金丸和富	髄液バイオマーカー	村山繁雄	アルツハイマー病診断	真興交易出版	東京	2006.7	121-126
石川智久，池田　学	臨床症状（地域コホート研究を基盤として）	村山繁雄	アルツハイマー病診断	真興交易出版	東京	2006.7	43-53
池田　学	認知症の診断	池上博司，楽木宏美	老年病・認知症ー長寿の秘けつー	メデイカルビュー社	東京	2006	207-211
池田　学	前頭側頭型痴呆に有効な薬物療法はあるか	上島国利，三村　将，中込和幸，平島奈津子	EBM精神疾患の治療2006-2007	中外医学社	東京	2006	363-367

池田　学	記憶障害	岩田　誠, 鹿島晴雄	言語聴覚士のための基礎知識　臨床神経学・高次脳機能障害学	医学書院	東京	2006	196-200
池田　学, 田辺敬貴	前頭側頭型認知症（痴呆）	平井俊作	老年期痴呆ナビゲーター	メデイカルビュー社	東京	2006	108-109
豊田泰孝, 池田　学	ピック病	平井俊作	老年期痴呆ナビゲーター	メデイカルビュー社	東京	2006	110-111
秦　龍二, 池田　学	FTDP-17	平井俊作	老年期痴呆ナビゲーター	メデイカルビュー社	東京	2006	118-119
Manabu Ikeda	Fronto-temporal dementia	Ritchie C W, Ames DJ, Masters CL, Cummings J	Therapeutic strategies in dementia	Clinical Publishing	Oxford	2006	287-299
池田　学	非アルツハイマー型変性認知症		今日の治療指針2008年版ー私はこう治療している	医学書院	東京	印刷中	
池田　学	前頭側頭型痴呆の治療法は	岡本幸市, 棚橋紀夫, 水澤英洋	EBM神経疾患の治療2006-2007	中外医学社	東京	2007	223-227
栗崎博司	神経心理検査(MMSE, HDS-R, WMS-R, WAIS-R, FAB, SDS) -もの忘れ外来での，神経心理検査の意味-	村山繁雄	アルツハイマー病診断	真興交易出版	東京	2006.7	54-71

松田博史	画像(SPECT,MRI)	村山繁雄	アルツハイマー病診断	真興交易出版	東京	2006.7	88-105
小尾智一	認知症を伴うパーキンソン病、レヴィー小体型認知症	村山繁雄	アルツハイマー病診断	真興交易出版	東京	2006.7	167-186
高尾昌樹, Ghetti B	FTDP-17とPick病	村山繁雄	アルツハイマー病診断	真興交易出版	東京	2006.7	187-198
大平雅之, 高尾昌樹	てんかん重積状態の管理方法は	岡本幸一, 棚橋紀夫 水沢英洋	EBM　神経疾患の治療	中外医学社	東京	2007.1	515-518
永島隆秀, 高尾昌樹, 濱田潤一	頭蓋内圧亢進・脳浮腫徴候	篠原幸人	神経救急・集中治療ハンドブック	医学書院	東京	2006.7	106-111

付.　　当該年度別刷

Available online at www.sciencedirect.com
SCIENCE DIRECT®
Neuroscience Research 54 (2006) 24–29
Neuroscience Research
www.elsevier.com/locate/neures

Beta-site APP cleaving enzyme 1 (BACE1) is increased in remaining neurons in Alzheimer's disease brains

Hirotsugu Harada [a], Akira Tamaoka [a,*], Kazuhiro Ishii [a], Shin'ichi Shoji [a], Satoshi Kametaka [b], Fuyuki Kametani [c], Yuko Saito [d], Shigeo Murayama [d]

[a] *Department of Neurology, Institute of Clinical Medicine, University of Tsukuba, 1-1-1 Tennodai, Tsukuba, Ibaraki 305-8575, Japan*
[b] *Osaka University, Osaka, Japan*
[c] *Tokyo Institute of Psychiatry, Tokyo, Japan*
[d] *Tokyo Metropolitan Institute of Gerontology, Tokyo, Japan*

Received 19 July 2005; accepted 11 October 2005
Available online 11 November 2005

Abstract

Alzheimer's disease (AD) is characterized by the extensive deposition of amyloid β protein (Aβ) in the brain cortex. Aβ is produced from β-amyloid precursor protein (APP) by β-secretase and γ-secretase. β-Secretase has been identified as beta-site APP cleaving enzyme1 (BACE1). We produced rabbit polyclonal antibodies against the amino and the carboxyl terminals of BACE1. Using these antibodies, BACE1 was characterized in temporal lobe cortices by Western blotting and immunohistochemistry.

Immunohistochemical studies employing anti-GFAP and anti-MAP2 antibodies as well as anti-BACE1 antibodies showed that BACE1 was expressed exclusively in neurons but not in glial cells.

Brain samples were directly extracted by 0.5% SDS and analyzed by Western blotting and densitometer. Although the mean level of BACE1/mg protein in AD brains was not increased, the ratio of BACE1 to MAP2 or to NSE was significantly increased compared with that in control brains.

Taken together, these findings suggest that those neurons that survive in AD brains might generate more BACE1 than normal neurons in control brains, indicating that increased BACE1 activity could be one of the causes of AD. This could justify the development of anti-BACE1 drugs for AD treatment.

Keywords: Alzheimer's disease; Aβ; BACE1

1. Introduction

Alzheimer's disease (AD) is a major form of senile dementia. The appearance of senile plaques with β-amyloid protein (Aβ) as the main component precedes the various pathological changes observed in AD brains (Glenner and Wong, 1984). Aβ is produced by cleavage of Aβ precursor protein (APP) at the amino terminal end by β-secretase and at the carboxyl terminal end by γ-secretase (Hardy and Allsop, 1991). Part of the Aβ released outside the cell is degraded and removed by degradative enzymes; however, increased Aβ production, reduced activity of the degradative enzymes, or reduced activity of the mechanism for removal of Aβ causes the formation of senile plaques through the aggregation and deposition of Aβ (Selkoe, 1999). Furthermore, aggregated Aβ acts against neuronal cells and causes neuronal cell death. It is also said that Aβ activates the phosphorylation of tau protein, causing neurofibrillary degeneration (Rapoport et al., 2002; King, 2005). Therefore, it is considered that inhibition of Aβ production before its deposition, enhancement of Aβ degradation, or clearance of deposited Aβ would be effective in the prevention and treatment of AD. Two phenotypes of BACE have been observed: BACE1 and BACE2. BACE1 is considered to be the major β-secretase because: (1) it exists mainly in the brain, whereas BACE2 is widely distributed throughout the body; (2) only small amounts of BACE2 mRNA have been observed in the brain (Vassar et al., 1999; Bennett et al., 2000; Vassar, 2004). Furthermore, although Aβ production is

* Corresponding author. Fax: +81 29 853 3224.
E-mail addresses: haradah@nona.dti.ne.jp (H. Harada), atamaoka@md.tsukuba.ac.jp (A. Tamaoka).

0168-0102/$ – see front matter
doi:10.1016/j.neures.2005.10.001

increased when human BACE1 is overexpressed in transgenic mice that express a Swedish variant of APP, it is not observed in BACE1 knockout mice (Bodendorf et al., 2002; Luo et al., 2001). These findings suggest that BACE1 inhibitors would suppress the production of Aβ and might be useful as new therapies for AD. To study the localization of BACE1 in AD brains, we prepared anti-human BACE1 antibodies and investigated their reactivity and specificity. We also compared the quantities of BACE1 between normal and AD brains. In addition, we analyzed the relationship between the amount of BACE1 and Aβ species, as measured by enzyme-linked immunosorbent assay (ELISA).

2. Methods

2.1. Case selection

We used frozen temporal lobe cortices (Brodmann area 21) preserved in this hospital and at the Tokyo Metropolitan Institute of Gerontology, including 28 AD cases and 25 normal controls. All AD cases had been diagnosed pathologically according to the criteria of the Reagan Institute Working Group/National Institute on Aging (stages 5 and 6 according to Braak and Braak) (Braak and Braak, 1991; The National Institute on Aging, and Reagan Institute Working Group on Diagnostic Criteria for the Neuropathological Assessment of Alzheimer's Disease, 1997), having been clinically and pathologically differentiated from dementia caused by other diseases. All control subjects had been examined clinically and pathologically. Their causes of death were cerebrovascular infarction or non-neurological diseases. The temporal, frontal, occipital, and parietal lobes from the control brains had been confirmed as pathologically normal for age. No significant differences between AD and control cases were evident concerning distributions of age, gender, or postmortem interval (range, 3–12 h).

2.2. Cultured cells as positive controls expressing human BACE1

pcDNA3-hBACE1 was prepared by cloning full-length BACE1 from the human brain library and then inserting pcDNA3. Next, the construct was transiently forced to express itself in HeLa cells and treated in a lysis buffer (10 mM Tris–HCl [pH 8.0], 150 mM NaCl, 1% NP40, 1% Triton-X100, 2 mM EDTA, protease inhibitor cocktail [Roche, Penzberg, Germany], 1 mM PMSF) on ice for 30 min. The resultant solution was centrifuged at 100 000 × *g* for 15 min to obtain the lysate, the supernatant of this process.

2.3. Preparation of antibodies

Rabbits were immunized with synthetic peptides of the amino terminal (45–55, ETDEEPEEPGR) and the carboxyl terminal (485–501, CLRQQHDDFADDISLLK) of BACE1 to prepare polyclonal antibodies, referred to here as anti-BACE1-N antibody and anti-BACE1-C antibody, respectively.

2.4. Preparation of brain samples and Western blotting

To determine the solubility of BACE1, brain samples were homogenized in a buffer (described below) with three times the volume of the sample, and the whole homogenate was then centrifuged at 100 000 × *g* for 20 min to separate the supernatant. Consecutive extraction was performed with TSE (10 mM Tris–HCl, 150 mM NaCl, 1 mM EDTA), 0.1% Triton-X100/TSE, and 0.5% SDS/TSE, which were added with the inhibitors of proteolytic enzymes (Roche).

The samples of each supernatant and the final pellets were heat-blocked for 10 min in a loading buffer (125 mM Tris–HCl, 20% glycerol, 10% 2-mercaptethanol, 4% SDS, 0.02% bromophenol blue, pH 6.8) and then subjected to electrophoresis on a 10–20% Tris–glycine sodium dodecyl sulfate–polyacrylamide gel (Real Gel Plate, Biocraft, Tokyo, Japan). The samples were then electrically transferred to a transfer membrane (Millipore, Billerico, MA) and blocked for 1 h in phosphate buffered saline (PBS) containing 10% skim milk and 0.1% Tween 20. Anti-BACE1-N antibody (1:2000) and anti-BACE1-C antibody (1:5000) were incubated at 4 °C overnight in a PBS buffer containing 5% bovine albumin. The membrane was rinsed with PBS buffer containing 0.1% Tween 20, incubated with HRP-labeled anti-rabbit IgG (1:5000, Dako-Cytomation, Glostrup, Denmark) for 3 h, and then stained with the detection reagents (Amersham, Buckinghamshire, UK).

Subsequently, direct extraction of a control brain was performed with 0.5% SDS/TSE, which could dissolve more proteins than the other two buffers (TSE or 0.1% Triton-X100/TS), and Western blotting was performed by using 1132-N (1:1000) and 1134-C (1:1000) as authentic BACE1 antibodies against amino acids 45–56 and 487–501, respectively, in addition to anti-BACE1-N antibody (1:2000) and anti-BACE1-C antibody (1:5000).

To study post-translational glycosidation of BACE1, control brain extracts with 0.5% SDS/TSE were incubated at 37 °C for 14 h using an N-Glycosidase F Deglycosylation Kit (Roche), and Western blotting was performed by using anti-BACE1-N antibody and anti-BACE1-C antibody.

To compare total quantities of BACE1, the brains of the 25 normal controls and 28 AD patients were extracted with 0.5% SDS/TSE. After protein amounts were measured by the bicinchoninic acid method (PIERCE, Rockford, IL), concentrations of protein in each sample were adjusted to be equal. Anti-BACE1-C antibody (1:5000), anti-microtubule-associated protein 2 (MAP2) antibody (Sigma, St. Louis, MO), and anti-neuron specific enolase (NSE) antibody (IBL, Gunma, Japan) were used as the primary antibodies, and HRP-labeled anti rabbit antibody was used as the secondary antibody for Western blotting. Measurement and comparison were performed with a densitometer (GS-710, Quantity One, Bio-Rad, Richmond, CA).

2.5. Double immunostaining

Double immunostaining was performed on 6-μm-thick paraffin sections of the temporal lobes from AD brains. After deparaffinization, blocking was performed using PBS containing 5% goat serum and 0.1% Tween 20, then staining was performed with anti-BACE1-C antibody (1:500) as the primary antibody and anti-rabbit IgG (H + L) Fluor 488 (1:400, Molecular Probes Europe BV, Leiden, The Netherlands) as the secondary antibody. Double staining was then performed using anti-MAP2 antibody and anti-GFAP antibody (Progen, Heidelberg, Germany) as the first antibodies and anti-mouse IgG (H + L) Fluor 633 (Molecular Probes Europe BV) as the second antibody. Confocal images were obtained under a confocal laser microscope (TCS SP2, Leica Microsystems, Wetzlar, Germany).

2.6. Quantification of Aβ by sandwich-type enzyme-linked immunosorbent assay (ELISA)

Species of Aβ were measured using the same parts of the temporal lobe cortices that had been used to measure BACE1. Wet tissue (0.5 g) from the cortex of each patient was finely minced, homogenized in 2 ml of 99% formic acid, and centrifuged at 100 000 × *g* for 60 min at 4 °C. The supernatant was neutralized with 1N NaOH, diluted, and subjected to ELISA for Aβ quantitation. To immunochemically identify and quantify different species of Aβ in the cortex, we used a sandwich ELISA with BA27 and BC05, which respectively are HRP-labeled antibodies capable of distinguishing the differing COOH-termini of Aβ 1–40 and 1–42. The sandwich ELISA for Aβ was carried out as described previously (Tamaoka et al., 1995, 1997). Briefly, 100 μl of a standard peptide to establish antibody specificity or a prepared patient sample was placed in a microtiter plate wells previously coated with BNT77, a monoclonal antibody against the NH_2-terminal sequence of Aβ (1–16). Samples were allowed to react at 4 °C for 24 h. After washing with PBS, plates were incubated at 4 °C for 24 h with wells containing HRP-labeled BA27 or BC05, the secondary antibodies for differential measurement of Aβ 40 and Aβ 42, respectively. HRP activities bound to antibodies reacting with samples were assayed with a microtiter plate reader after color development using the TMB microwell peroxidase system (KPL, Gaithersburg, MD).

3. Results

3.1. A 70-kDa protein is detected in the cerebral cortex by anti-BACE1-C antibody and anti-BACE1-N antibody

Supernatants of consecutive extractions from the temporal cortex, final pellets, and positive controls were analyzed on immunoblots with anti-BACE1-C antibody and anti-BACE1-N antibody. Fractions consecutively extracted with TSE, 1% Triton-X100/TSE, and 0.5% SDS/TSE revealed a band migrating at ~70 kDa in all supernatants; however, no band was observed at the same position in the final pellet (Fig. 1a). Since each consecutively extracted fraction contained ~70 kDa protein, Western blotting was performed thereafter on prepared samples obtained by direct extraction of brains with 0.5% SDS/TSE. All these antibodies detected a band migrating at 70 kDa in such fractions (Fig. 1b).

We considered that we had identified mature BACE1, because we observed a band at 70 kDa with both the anti-BACE1-N antibody and the anti-BACE1-C antibody, and it comigrated with a protein with the molecular weight of BACE1, as already reported (Haniu et al., 2000). Deglycosylation of the positive controls with N-glycosidase F resulted in disappearance of the band at 70 kDa and appearance of a band at 50 kDa. Thus, the full-length mature BACE1 was confirmed as the glycosylated form of BACE1 (Fig. 2). Western blotting of control brains with anti-BACE1-C antibody and anti-BACE1-N antibody revealed a band at the same position as the deglycosylated form of BACE1 after treatment with N-glycosidase F.

3.2. BACE1 is expressed mainly in neurons

To determine whether expression of BACE1 in the AD brain occurred mainly in neurons or in astrocytes accompanying the gliosis, we performed double immunostaining of the temporal lobes of AD and normal brains. Stainings of the cortices of the temporal lobe and the hippocampus against anti-BACE1-C antibody were consistent with those for anti-MAP2 antibody. Astrocytes stained for anti-GFAP antibody were not labeled by anti-BACE1-C antibody (Fig. 3). These findings led us to consider that BACE1 was expressed mainly in the neurons, not in glial cells.

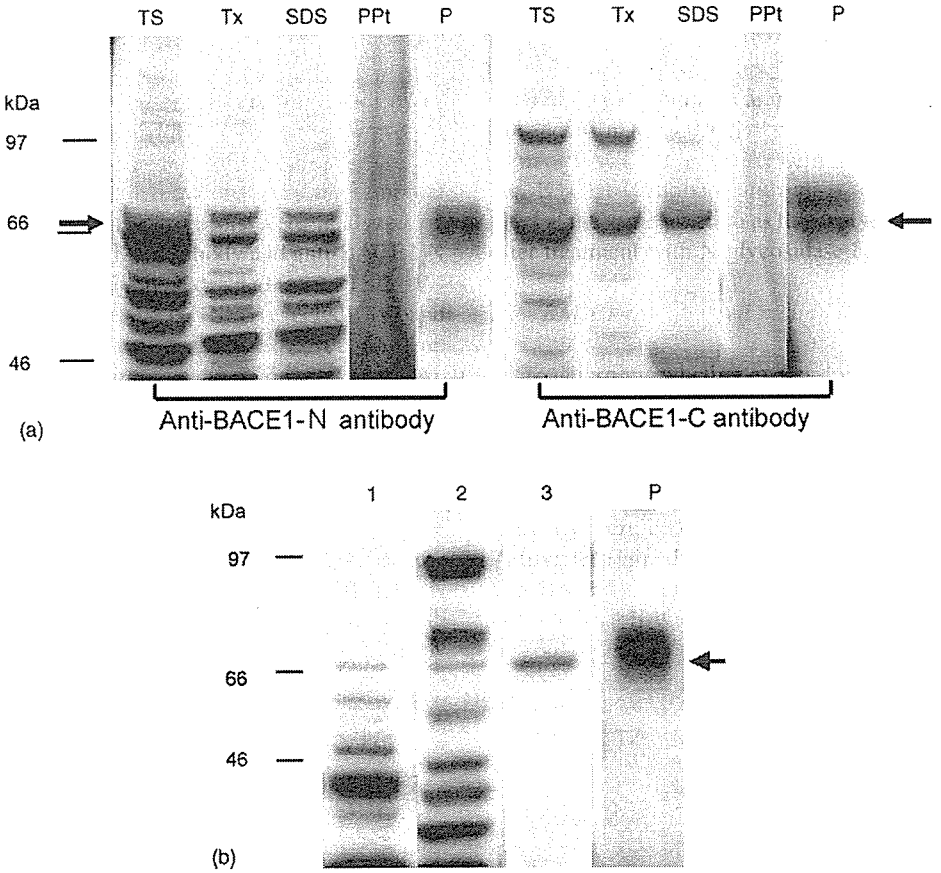

Fig. 1. (a) Immunoblots of sequential extractions of control brain stained with anti-BACE1-N antibody (left) and anti-BACE1-C antibody (right). The acrylamide gel gradient was 10–20%. Lanes: TS, supernatant directly extracted by TSE; Tx, supernatant sequentially extracted by 1% Triton-X100/TSE; SDS, supernatant sequentially extracted by 0.5% SDS/TSE; PPt, final pellet; P, positive control. All brain fractions extracted sequentially by TS, Tx, and SDS were revealed to contain 70 kDa protein (arrow), but PPt did not. (b) Immunoblots of supernatant directly extracted by 0.5% SDS from control brain stained with various anti-BACE1 antibodies. The acrylamide gel gradient was 10–20%. Lanes: 1, 1132-N (1:1000); 2, 1134-C (1:1000); 3, anti-BACE1-N antibody (1:2000); 4, anti-BACE1-C antibody (1:5000); P, positive control stained with anti-BACE1-C antibody. All antibodies detected 70-kDa protein (arrow).

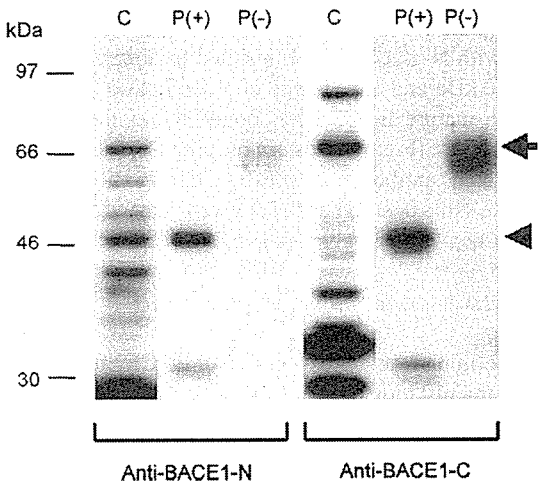

Fig. 2. Immunoblots of recombinant BACE1 (positive control) digested by N-glycosidase F. Lanes; C, supernatant directly extracted by 0.5% SDS from a control brain (untreated); P(+), positive control digested by N-glycosidase F; P(−), untreated positive control. Digestion of positive control by N-glycosidase F altered the molecular weight from 70 (arrow) to 50 kDa (arrowhead), which was consistent with the molecular weight of BACE1 calculated from its amino acid residues. The 70- and 50-kDa bands were also detected in immunoblots of a control brain with anti-BACE1-N antibody (left) and anti-BACE1-C antibody (right).

3.3. BACE1 expression is increased in remaining neurons in AD brains

Because double immunostaining suggested that BACE1 was expressed mainly in neurons, we performed Western blotting with anti-BACE1-C antibody as well as with anti-MAP2 antibody and anti-NSE antibody, measuring the amounts of these proteins (Fig. 4). There were no significant differences in the total amounts of BACE1 between AD and control brains. However, significant decreases in the levels of MAP2 and NSE were observed in the AD group compared with the normal group: the amount of MAP2 in the AD group as a proportion of that in the normal group was 0.29 ($p < 0.05$), and that of NSE was 0.31 ($p < 0.001$). These results were assumed to reflect neuronal loss in the AD brains. The ratios of BACE1 to MAP2 (BACE1/MAP2) and NSE (BACE1/NSE) were 3.0 and 4.6 (both $p < 0.05$), respectively, in the AD group (Fig. 5). We considered that these ratios reflected the relative amounts of BACE1 per neuron. There was a tendency towards an increase in BACE1 concentration with age in both groups, although this trend was not significant. This tendency was greater in AD brains than in the controls (data not shown).

Sandwich ELISA showed that the levels of both Aβ 40 and Aβ 42 were increased in the AD group, as shown previously

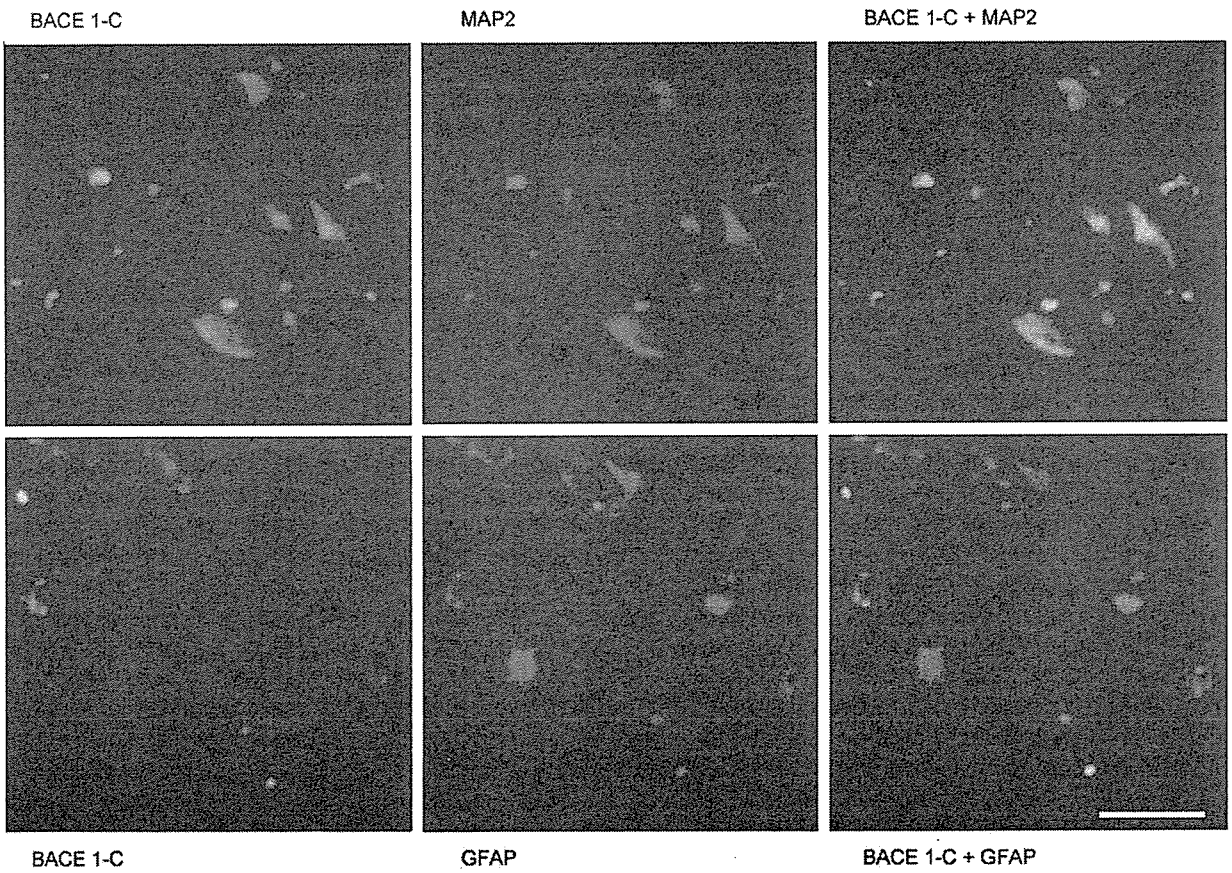

Fig. 3. Immunohistochemical studies of temporal cortex from AD brain, employing anti-MAP2 antibody (upper row, red) and anti-GFAP antibody (lower row, red) as well as anti-BACE1-C antibody (green). BACE1 was expressed exclusively in neurons but not in astrocytes (bar = 40 μm).

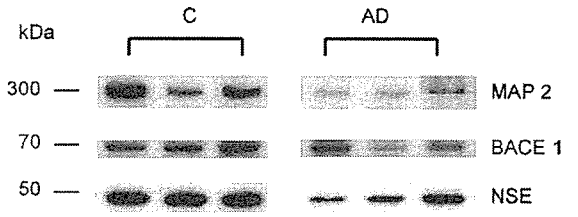

Fig. 4. Western blottings using anti-BACE1-C antibody, anti-MAP2, and anti-NSE in AD and control brains. The samples were extracted with 0.5% SDS/TSE and the concentration of protein in each sample was adjusted to the same level.

(Tamaoka et al., 1995); however, we observed no correlation between the concentrations of BACE1 and Aβ species.

4. Discussion

BACE1 is first synthesized as a transmembrane protein with 501 amino acids. The 1–21 amino acid part of the protein represents a signal peptide and the adjacent 22–45 part represents a proprotein domain. The remaining 46–501 part is considered to undergo maturation through endoplasmic reticulum to become the final 70 kDa mature BACE1 (Vassar et al., 1999; Haniu et al., 2000; Vassar, 2004). Several findings support the identity of the 70-kDa protein recognized by our antibodies as BACE1. (i) In addition to our two antibodies (anti-BACE1-N and anti-BACE1-C), 1132-N and 1134-C, polyclonal antibodies against carboxyl-terminal of BACE1, also detected the same 70-kDa protein band. (ii) Few numbers of extrabands were observed in the Western blottings using anti-BACE1-C antibody in AD and control brains. (iii) Both our novel antibodies against BACE1 immunostained recombinant BACE1 as the band migrating at 70 kDa and deglycosylated recombinant BACE1 at 50 kDa, which is consistent with the molecular weight of BACE1 calculated from its amino acid composition. In the light of the molecular weight of BACE1 calculated by its amino acid composition, with 46–501 amino acid residues, we considered the 50 kDa band that appeared after treatment with N-glycosidase F in the positive controls to be deglycosylated BACE1. The same deglycosylated forms of BACE1 could be identified in normal brains. These findings implied that unmodified BACE1 was present in human brains.

Expression of BACE1 was confirmed by double immunofluorescence staining to occur exclusively in the neurons, as reported previously (Seubert et al., 1993; Zhao et al., 1996). Therefore, we measured the amount of BACE1 protein as well as the amounts of MAP2 and NSE, as neuron-specific proteins, and then examined the ratios of BACE1/MAP2 and BACE1/NSE, which we considered to reflect the level of BACE1 expression per neuron.

We concluded that BACE1 expression per neuron was increased, although the total amount of BACE1 expression in the cortices of the temporal lobe was not increased. This observation implied that Aβ production per neuron might increase before cell death. Fukumoto et al. reported that the total amount of BACE1 protein in the temporal lobes of AD brains tended to increase, as measured by sandwich ELISA using mouse monoclonal anti BACE1 carboxyl terminal antibody and rabbit polyclonal anti BACE1 amino terminal antibody. From the amount of synaptophysin, as measured by ELISA, they also reported that BACE1 expression per neuron was increased in AD brains, because the value of the amount of BACE1 divided by the amount of synaptophysin was increased (Fukumoto et al., 2002). There results are fairly consistent with ours.

Yang et al. reported elevated BACE1 expression and activity in sporadic AD. By using Western blotting analysis they showed that BACE1 levels were significantly higher in the temporal cortex in AD than in non-demented controls. The

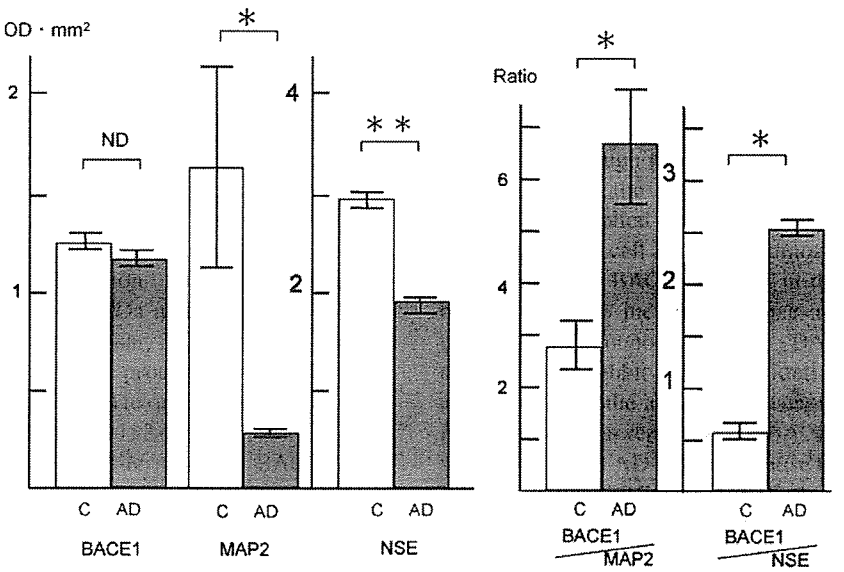

Fig. 5. Protein levels of BACE1, MAP2, and NSE in AD and control (C) brains. The amount of BACE1/mg protein in AD brains was slightly decreased in comparison with that in control brains. However, in AD, the ratios of BACE1 to MAP2 (BACE1/MAP2) and BACE1 to NSE (BACE1/NSE) were significantly increased compared with those in control brains (BACE1/MAP2 and BACE1/NSE $p < 0.05$) ($^{*}p < 0.05$; $^{**}p < 0.0001$).

differences in results between their study and ours could be due to several factors. (i) They used rapidly autopsied brains of AD patients (<3 h), although they did not comment on the postmortem intervals of the non-demented controls. (ii) They normalized BACE1 expression against β-actin. (iii) The AD brain samples that they used might have contained quite large quantities of neurons, as suggested by their levels of MAP-2 and NSE expression. Further studies using brains examined after different postmortem intervals and samples from different brain lesions are needed before we can draw definite conclusions on BACE1 expression (Yang et al., 2003).

Production of Aβ is not seen in BACE1 knockout mice, and no abnormalities are observed in these mice (Luo et al., 2001; Roberds et al., 2001). On the other hand, γ-secretase, which is the cleavage enzyme at the carboxyl terminal side of APP, is also involved in the cleavage of other proteins such as Notch1. Notch1 is an important substance involved in the differentiation and transportation of cells during the embryonic period. It is also known that Notch1 is involved in the differentiation of immune cells in the body, and that inhibition of its cleavage activity causes immune abnormalities (Petit et al., 2001). Therefore, we consider that reduction in the amount of BACE1 is less likely to cause side effects than targeting of γ-secretase.

Several lines of evidence have led to postulation that Aβ accumulation comes from enhancement of its production, promotion of its aggregation, or inhibition of its degradation or excretion (Selkoe, 1999; Hardy and Selkoe, 2002; Iwata et al., 2001). Our results revealed no correlation between the amount of BACE1 protein and the accumulated amount of Aβ species, suggesting that several other factors could cause abnormal accumulation of Aβ in the AD brain. However, BACE1 inhibitors could still provide a new therapy for AD, possibly through inhibition of additional production of Aβ. This is supported by the fact that our study revealed increased production of BACE1 by the surviving neurons in AD brains, and by a previous report that Aβ production is not detected in BACE1 knockout mice.

Acknowledgments

This work was supported in part by Grants-in-Aid to A.T. from the Ministry of Education, Culture, Sports, Science and Technology and from the Ministry of Health, Labour and Welfare.

References

Bennett, B.D., Babu-Khan, S., Loeloff, R., Louis, J.C., Curran, E., Citron, M., Vassar, R., 2000. Expression analysis of BACE2 in brain and peripheral tissues. J. Biol. Chem. 275, 20647–20651.

Bodendorf, U., Danner, S., Fischer, F., Stefani, M., Sturchler-Pierrat, C., Wiederhold, K.H., Staufenbiel, M., Paganetti, P., 2002. Expression of human beta-secretase in the mouse brain increases the steady-state level of beta-amyloid. J. Neurochem. 80, 799–806.

Braak, H., Braak, E., 1991. Neuropathological stageing of Alzheimer-related changes. Acta Neuropathol. (Berlin) 82, 239–259.

Fukumoto, H., Cheung, B.S., Hyman, B.T., Iraozarry, M.C., 2002. β-Secretase protein and activity are increased in the neocortex in Alzheimer disease. Arch. Neurol. 59, 1381–1389.

Glenner, G.G., Wong, C.W., 1984. Alzheimer's disease: initial report of the purification and characterization of a novel cerebrovascular amyloid protein. Biochem. Biophys. Res. Commun. 120, 885–890.

Haniu, M., Denis, P., Young, Y., Mendiaz, E.A., Fuller, J., Hui, J.O., Bennett, B.D., Kahn, S., Ross, S., Burgess, T., Katta, V., Rogers, G., Vassar, R., Citron, M., 2000. Characterization of Alzheimer's beta-secretase protein BACE. A pepsin family member with unusual properties. J. Biol. Chem. 275, 21099–21106.

Hardy, J., Allsop, D., 1991. Amyloid deposition as the central event in the aetiology of Alzheimer's disease. Trends Phamac. 12, 383–388.

Hardy, J., Selkoe, D.J., 2002. The amyloid hypothesis of Alzheimer's disease: progress and problems on the road to therapeutics. Science 297, 353–356.

Iwata, N., Tsubuki, S., Takaki, Y., Shirotani, K., Lu, B., Gerard, N.P., Gerard, C., Hama, E., Lee, H.J., Saido, T.C., 2001. Metabolic regulation of brain Abeta by neprilysin. Science 292, 1550–1552.

King, M.E., 2005. Can tau filaments be both physiologically beneficial and toxic? Biochim. Biophys. Acta 1739, 260–267.

Luo, Y., Bolon, B., Kahn, S., Bennett, B.D., Babu-Khan, S., Denis, P., Fan, W., Kha, H., Zhang, J., Gong, Y., Martin, L., Louis, J.C., Yan, Q., Richards, W.G., Citron, M., Vassar, R., 2001. Mice deficient in BACE1, the Alzheimer's beta-secretase, have normal phenotype and abolished beta-amyloid generation. Nat. Neurosci. 4, H231–H232.

Petit, A., Bihel, F., Alves da Costa, C., Pourquie, O., Checler, F., Kraus, J.L., 2001. New protease inhibitors prevent gamma-secretase-mediated production of Abeta 40/42 without affecting Notch cleavage. Nat. Cell Biol. 3, 507–511.

Rapoport, M., Dawson, H.N., Binder, L.I., Vitek, M.P., Ferreira, A., 2002. Tau is essential to beta-amyloid-induced neurotoxicity. Proc. Natl. Acad. Sci. U.S.A. 99, 6364–6369.

Roberds, S.L., Anderson, J., Basi, G., Bienkowski, M.J., Branstetter, D.G., Chen, K.S., Freedman, S.B., Frigon, N.L., Games, D., Hu, K., Johnson-Wood, K., Kappenman, K.E., Kawabe, T.T., Kola, I., Kuehn, R., Lee, M., Liu, W., Motter, R., Nichols, N.F., Power, M., Robertson, D.W., Schenk, D., Schoor, M., Shopp, G.M., Shuck, M.E., Sinha, S., Svensson, K.A., Tatsuno, G., Tintrup, H., Wijsman, J., Wright, S., McConlogue, L., 2001. BACE knockout mice are healthy despite lacking the primary beta-secretase activity in brain: implications for Alzheimer's disease therapeutics. Hum. Mol. Genet. 10, 1317–1324.

Selkoe, D.J., 1999. Translating cell biology into therapeutic advances in Alzheimer's disease. Nature 399, A23–A31.

Seubert, P., Oltersdorf, T., Lee, M.G., Barbour, R., Blomquist, C., Davis, D.L., Bryant, K., Fritz, L.C., Galasko, D., Thal, L.J., et al., 1993. Secretion of beta-amyloid precursor protein cleaved at the amino terminus of the beta-amyloid peptide. Nature 361, 260–263.

Tamaoka, A., Sawamura, N., Fukushima, T., Shoji, S., Matsubara, E., Shoji, M., Hirai, S., Furiya, Y., Endoh, R., Mori, H., 1997. Amyloid beta protein 42 (43) in cerebrospinal fluid of patients with Alzheimer's disease. J. Neurol. Sci. 148, 41–45.

Tamaoka, A., Sawamura, N., Odaka, A., Suzuki, N., Mizusawa, H., Shoji, S., Mori, H., 1995. Amyloid beta protein 1–42/43 (Abeta 1–42/43) in cerebellar diffuse plaques: enzyme-linked immunosorbent assay and immunocytochemical study. Brain Res. 679, 151–156.

The National Institute on Aging, and Reagan Institute Working Group on Diagnostic Criteria for the Neuropathological Assessment of Alzheimer's Disease, 1997. Consensus recommendations for the postmortem diagnosis of Alzheimer's disease. Neurobiol. Aging 18, S1–S2.

Vassar, R., 2004. BACE1: the beta-secretase enzyme in Alzheimer's disease. J. Mol. Neurosci. 23, 105–114.

Vassar, R., Bennett, B.D., Babu-Khan, S., 1999. β-Secretase cleavage of Alzheimer's amyloid precursor protein by the transmembrane aspartic protease BACE. Science 286, 735–741.

Yang, L.B., Lindholm, K., Yan, R., Citron, M., Xia, W., Yang, X.L., Beach, T., Sue, L., Wong, P., Price, D., Li, R., Shen, Y., 2003. Elevated beta-secretase expression and enzymatic activity detected in sporadic Alzheimer disease. Nat. Med. 9, 3–4.

Zhao, J., Paganini, L., Mucke, L., Gordon, M., Refolo, L., Carman, M., Sinha, S., Oltersdorf, T., Lieberburg, I., McConlogue, L., 1996. Beta-secretase processing of the beta-amyloid precursor protein in transgenic mice is efficient in neurons but inefficient in astrocytes. J. Biol. Chem. 271, 31407–31411.

Available online at www.sciencedirect.com
SCIENCE DIRECT
ELSEVIER
Neuroscience Research 54 (2006) 197–201
Neuroscience Research
www.elsevier.com/locate/neures

Increased levels of granular tau oligomers: An early sign of brain aging and Alzheimer's disease

Sumihiro Maeda [a,b], Naruhiko Sahara [a], Yuko Saito [c], Shigeo Murayama [c], Atsushi Ikai [b], Akihiko Takashima [a,*]

[a] *Lab for Alzheimer's Disease, Brain Science Institute, RIKEN, 2-1 Hirosaswa, Wako, Saitama 351-0198, Japan*
[b] *Department of Life Science, Graduate School of Bioscience and Biotechnology, Tokyo Institute of Technology, 4259 Nagatsuda, Midori-Ku, Yokohama, Kanagawa 226-8501, Japan*
[c] *Department of Neuropathology, Tokyo Metropolitan Institute of Gerontology, 35-2 Sakaecho, Itabashi-ku, Tokyo 173-0015, Japan*

Received 2 November 2005; accepted 25 November 2005
Available online 6 January 2006

Abstract

Development of neurofibrillary tangles (NFTs) is a pathological hallmark in various neurodegenerative disorders including Alzheimer's disease (AD). Recently, we identified a granular tau oligomer having a pre-filamentous structure. To determine the role of this oligomer in NFT formation, we quantified the amount of granular tau oligomer in 21 frontal cortex samples, each displaying varying degrees of Braak-staged NFT pathology. Here we report that granular tau oligomer levels in frontal cortex were significantly increased, even in brains displaying Braak-stage I neuropathology, a stage at which clinical symptoms of AD and NFTs in frontal cortex are believed to be absent. This suggests that increases in granular tau oligomer levels occur before NFTs form and before individuals manifest clinical symptoms of AD. Increased granular tau oligomer levels, therefore, may lead to NFT formation in frontal cortex, eventually leading to the development of AD. Thus, increases in granular tau oligomer levels may represent a very early sign of NFT formation and AD.

Keywords: Alzheimer's disease (AD); Tau; Atomic force microscopy (AFM); Granular tau oligomer; Braak stage; Brain aging

1. Introduction

Tau, a microtubule-associated protein, can aggregate into filamentous polymer forms (von Bergen et al., 2005). Bundled tau filaments that deposit in cells are called neurofibrillary tangles (NFTs), which commonly form in the brain during normal aging and in Alzheimer's disease (AD). In AD, NFTs and neuronal cell loss typically coincide within the same brain regions (Gomez-Isla et al., 1997). The progressively expanding anatomical distribution of NFTs reflects progressive brain dysfunction in disease, suggesting that NFT formation and neuronal cell loss may share a common mechanism (Ihara, 2001). The recent finding that patients with frontotemporal dementia and parkinsonism linked to chromosome 17 (FTDP-17) harbor tau mutations (Reed et al., 2001), strongly suggests that tau dysfunction itself can cause neurodegeneration. Indeed, the overexpression of tau in various animal models has been shown to induce neurodegeneration (Lee et al., 2001; Tanemura et al., 2001, 2002; Tatebayashi et al., 2002). However, others have observed that neuronal cell loss occurs disproportionately to the number of NFTs in AD (Gomez-Isla et al., 1997). Conversely, others have reported neuronal loss in the absence of NFTs in a tau-overexpressing *Drosophila* model (Wittmann et al., 2001), suggesting that the events that lead from tau accumulation to neurodegeneration may not involve filament formation. Recently, (Santacruz et al., 2005) reported that reducing tau overexpression in mutant tau transgenic mice decreased neuronal cell loss even though filaments continued to form, suggesting that filament formation may not be the underlying cause of neuronal cell loss. Therefore, tau may be involved in neuronal dysfunction even before NFTs are formed.

Using an in vitro tau aggregation system, we identified a granular-shaped pre-filamentous form of tau – the granular tau oligomer – composed of about 40 tau molecules (Maeda et al.,

* Corresponding author.
E-mail address: kenneth@brain.riken.go.jp (A. Takashima).

0168-0102/$ – see front matter
doi:10.1016/j.neures.2005.11.009

unpublished data). We found that increasing the concentration of granular tau oligomers in vitro causes them to convert into filaments. The breakdown of PHF into granular tau structure by continuous AFM imaging has also observed indicating that granular tau oligomer composes of filament in vivo. In the present study, to understand the relationship between the levels of granular tau oligomer and the progression of AD, we quantified the amount of granular tau oligomer in various brain samples, each histopathologically confirmed to display different Braak stages (Braak and Braak, 1991). We then compared the amounts of granular tau oligomer in each Braak-staged sample using atomic force microscopy (AFM). We found increased levels of granular tau oligomer in brain samples at Braak stage I, a stage indicative of pre-symptomatic AD. Granular tau oligomers were detected even in samples at Braak stage 0.

2. Materials and methods

2.1. Subjects

Frozen frontal cortex samples from 21 subjects, including 5 patients with AD (Murayama and Saito, 2004), were obtained from the Tokyo Metropolitan Institute of Gerontology (TMIG) (Saito et al., 2004). The brains from TMIG were staged histopathologically according to the Braak staging system (Braak and Braak, 1991).

2.2. Antibodies

Anti-paired helical filament antibody, PHF-1, was a kind gift from Dr. P. Davies (Albert Einstein College of Medicine, USA). Anti-tau antibody, JM, was raised against full-length recombinant tau (Takashima et al., 1998). Anti-tau antibody, Tau-c, was raised against tau c-terminus polypeptide (amino acids 422–438, according to the longest human tau isoform).

2.3. Purification of granular tau oligomers

Human brain samples (~12 g) were homogenized with three volumes of a buffer containing 10 mM Tris (pH 7.4), 800 mM NaCl, 1 mM EGTA, 10% sucrose, and protease inhibitors, and centrifuged at 27,000 × *g* for 20 min at 4 °C. CHAPS (Dojindo, Kumamoto, Japan) was added to the supernatant to a final concentration of 1% (w/v), then loaded into an immunoaffinity column (2 ml bed volume) containing anti-tau antibody JM. The column was washed with at least 400 ml of buffer containing 10 mM Tris (pH 7.4), 800 mM NaCl, 1 mM EGTA, and 1% CHAPS. After confirming that no aggregates remained in the wash solution, the column was eluted with 5 ml of 3M KSCN (Jicha et al., 1999). After exchanging the above buffer to a buffer containing 10 mM Tris (pH 7.4), 800 mM NaCl, and 1 mM EGTA with a NAP-10 column (Amersham Biosciences), we added *N*-lauroylsarcosine (Nacalai tesque, Kyoto, Japan) until achieving a final concentration of 1% (wt./vol.). After 2 h of incubation, 1 ml of sample was layered onto a sucrose step gradient (50, 40, 30, and 20% sucrose) and centrifuged for 2 h at 50 K rpm in a MLS50 rotor (Beckman Coulter) using an Optima MAX-E ultracentrifuge (Beckman Coulter) at 23 °C. We separated the samples into 1 ml fractions, from top to bottom (fractions 1–5), to eliminate contamination from lower fractions. We washed the bottom of tubes with buffer and saved the wash solution as fraction 6. We previously isolated granular tau oligomer from fraction 3 derived from either in vitro aggregated tau or human brain samples (Maeda et al., unpublished data). In the present study, we also found that the granular tau oligomer localized to fraction 3.

2.4. Western blot analysis

Granular tau oligomer fractions were concentrated by adding trichloroacetic acid to the fractions and setting the mixtures on ice for 2 h. The mixtures were then centrifuged at 20,000 × *g* at 4 °C, and supernatants were removed and dried in a SpeedVac Concentrator (SAVANT). Loading buffer was added to the dried granular tau oligomers, and this mixture was subjected to SDS-PAGE and subsequent immunoblotting with anti-tau antibody Tau-c.

Sarcosyl-insoluble fractions were prepared by solubilizing homogenized brain tissue (see above) in 1% sarcosyl for 2 h at 25 °C, then centrifuging at 50 K rpm in a TLA 55 rotor (Beckman Coulter) for 20 min. After removing the supernatant, loading buffer was added to the pellet, and the insoluble tau was subjected to SDS-PAGE and immunoblotting with PHF-1 antibody. Immunoreactivities were quantified with the software program Image Gauge (Fujifilm).

2.5. Atomic force microscopy

Samples were dropped onto freshly cleaved mica and left in place for 30 min prior to AFM assessment. After washing the mica with water, we examined the tau-containing samples in solution using a Nanoscope IIIa (Digital Instruments, Santa Barbara, CA, USA) set at tapping mode (Hansma et al., 1995). OMCL-TR400PSA (Olympus, Japan) was used as a cantilever. The resonant frequency was about 9 kHz.

We examined four different areas (2 μm × 2 μm each) of the mica surface covered with granular aggregates. These areas were analyzed with NIH-image 1.63 and summations of four different areas were demonstrated.

2.6. Statistical analysis

The significant difference between each Braak staging was tested with Mann–Whitney test. Data were analyzed with Prism 4 for Macintosh (Graphpad, San Diego, CA, USA).

3. Results

3.1. Purification of granular tau oligomers

We purified granular tau oligomers from human frontal cortices (Table 1) pathologically classified according to the Braak staging system (Braak and Braak, 1991) and examined the oligomers using AFM. Fig. 1 shows representative AFM images of cortex samples from a Braak-stage 0 brain (non-AD) and a Braak-stage V brain (AD). Although we detected granular tau oligomers in both of these samples, the number of oligomers in the Braak-stage V sample was much greater than that in the Braak-stage 0 sample. The size of granular tau oligomers ranged from 5 to 50 nm. The peak of granular tau oligomer was around 20 nm in diameter, which is similar with in vitro generated granular tau oligomer. And granular tau oligomers derived from in vivo and in vitro were recovered into same fraction in sucrose centrifugation, indicating the similar sedimentation coefficient between them. PHF-1 immunoreactivity and similar bands pattern with PHF-tau on immunoblotting (Fig. 2b and c, Maeda et al., unpublished data) suggested the hyperphosphorylation in granular tau oligomer.

3.2. Accumulation of granular tau oligomers during early stages of NFT formation

We quantified the number of granular tau oligomers in Braak-staged cortex samples examined with AFM using NIH-image 1.63 (Fig. 2a). In samples staged at Braak stage 0, a stage at which the brain does not contain NFTs, we detected some, albeit a few, granular tau oligomers. In samples staged at Braak stage I (i.e., neuropathology typically seen in normal brain

Table 1
Demographics and characteristics of cases

Number	Age (years)	Gender	PMT (h:min)	NFT[a]	Senile plaque
1	52	M	15:51	0	0
2	69	F	11:48	0	A
3	82	F	39:04	0	0
4	87	M	70:10	0	0
5	78	M	2:02	0	0
6	66	F	9:51	0	B
7	81	M	3:00	I	B
8	97	F	2:40	I	B
9	84	M	47:25	I	B
10	87	M	4:25	I	C
11	93	M	20:49	I	C
12	86	F	6:50	III	C
13	94	M	13:00	III	C
14	87	F	4:21	III	C
15	82	F	10:32	III	C
16	89	F	16:11	III	C
17	90	F	64:07	V	C
18	86	F	19:51	V	C
19	93	F	13:28	V	C
20	70	M	35:42	V	C
21	80	F	6:41	V	C

Abbreviations: PMT, postmortem time; NFT, neurofibrillary tangle; SP, senile plaque.
[a] NFTs and SPs were staged according to the neuropathology staging system of Braak and Braak (1991).

aging), a stage at which entorhinal cortex but not frontal cortex contains NFTs, the number of granular tau oligomers present significantly increased compared to that in the Braak-stage 0 samples ($P = 0.0173$). In samples staged at Braak stage III, a stage at which both limbic areas and entorhinal cortex contain NFTs, the number of granular tau oligomers present also significantly increased compare to that in the Braak-stage 0 samples ($P = 0.0087$). In samples staged at Braak stage V, a stage at which neocortex including frontal cortex contain NFTs, the number of granules increased again significantly compare to that in Braak-stage 0 samples ($P = 0.0087$). We observed no significant differences in the number of granular tau oligomers in stage I, III, and V samples.

We confirmed these results by using Western blotting to assess granular tau oligomer fractions and conventionally purified sarcosyl-insoluble tau fractions derived from Braak-staged frontal cortices (Fig. 2b and c, respectively). The Tau-c immunostaining intensity of tau bands derived from the granular tau oligomer fraction of Braak-stage 0 samples was faint (Fig. 2b). Nonetheless, in Braak-stage I, III, and V samples, we did detect tau smears displaying a immunostaining pattern characteristic of insoluble tau (Fig. 2b cf. PHF-1 immunostaining pattern in Fig. 2c) (Selkoe et al., 1982; Ihara et al., 1983; Greenberg and Davies, 1990). Linear regression analysis revealed a significant correlation between Tau-c immunoreactivity and the number of granular tau oligomers ($P < 0.0001$, $r^2 = 0.6336$). On the other hand, similar statistical analysis failed to reveal a correlation between PHF-1 immunoreactivity and the number of granular tau oligomers.

Taken together, these results indicate that granular tau oligomer levels begin to increase in pre-symptomatic stages of disease, suggesting that granular tau oligomers may form before NFTs are formed.

4. Discussion

4.1. Granular tau oligomer as a pre-symptomatic marker for AD

Using silver-stained human brain sections, Braak and Braak (1991) described seven stages (0–VI) of neuropathology that are now commonly used to stage the progression of neurodegenerative diseases. The Braak staging system is based on the density and distribution of agyrophilic NFTs in the brain (Braak and Braak, 1991). Stage 0 is characterized by the absence of NFTs. Stages I and II are termed transentorhinal stages, because they are characterized by the presence of NFTs in the transentorhinal region. Stages I and II are distinguished by the density of NFTs. Stages III and IV are termed limbic stages, because they are characterized by the presence of NFTs in the hippocampus as well as in the transentorhinal region. Stages V and VI are termed isocortical stages, because they are

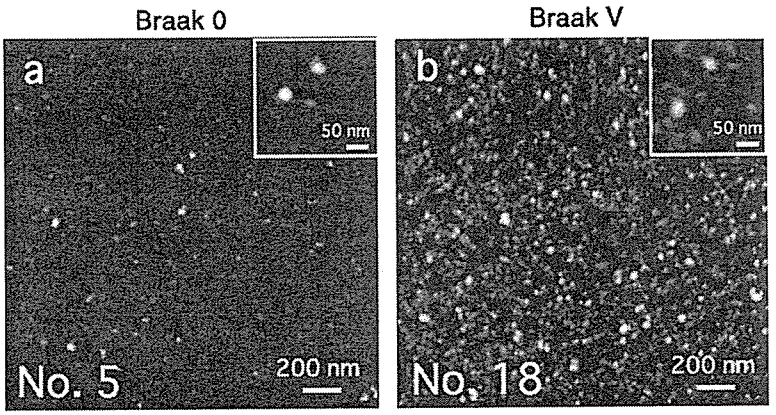

Fig. 1. Granular tau oligomers purified from human frontal cortex. Frontal cortex homogenates were fractionated with sucrose gradient centrifugation, and fractions (fraction 3) containing granular tau oligomers were examined in solution with AFM set to tapping mode. Representative data from the Braak-staged samples indicated are shown here. Insets contain high magnification AFM images of granular tau oligomers. The height range is 30 nm. The large numbers in the lower left corner of each panel correspond to the brain identification numbers in Table 1.

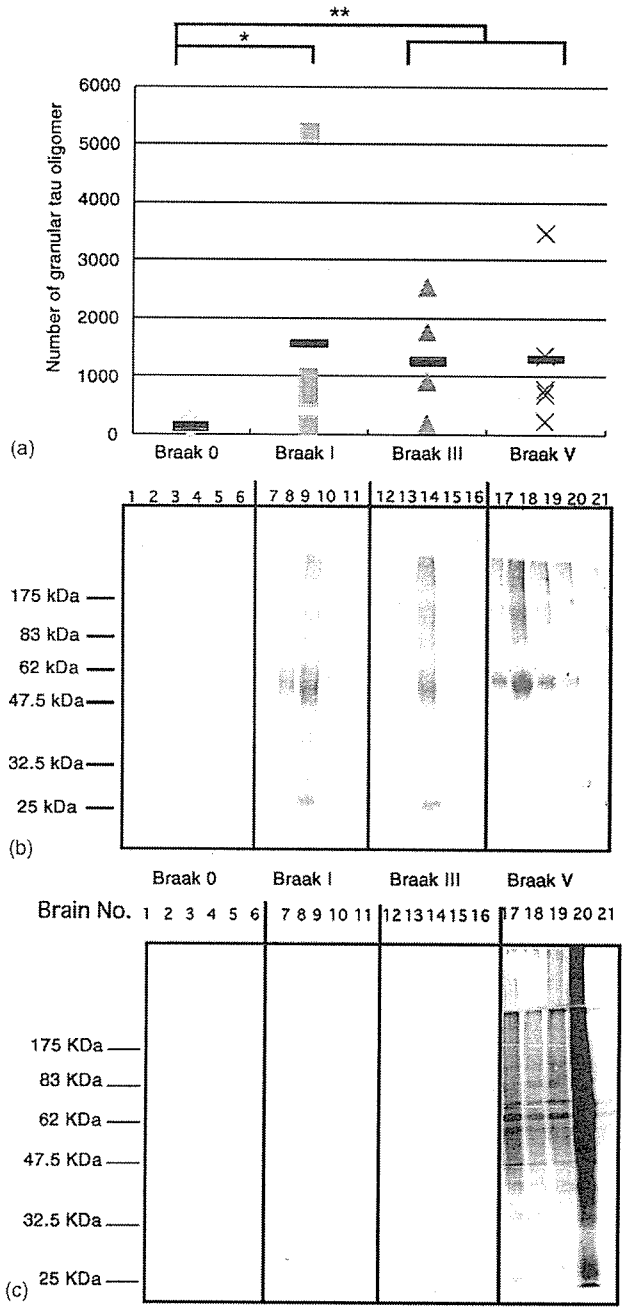

Fig. 2. The distribution of granular tau oligomers observed in different Braak stages. (a) AFM images of Braak-staged frontal cortex samples were analyzed with NIH-image 1.63, and the total number of granular aggregates in each sample were counted and graphed. $^{*}P < 0.05$, $^{**}P < 0.01$. (b) Western blots of fractions containing granular tau oligomers immunostained with Tau-c antibody. (c) Western blots of sarcosyl-insoluble fractions immunostained with PHF-1 antibody for the detection of tau filaments.

characterized by the extension of NFTs into neocortex, including frontal cortex.

The density and distribution of NFTs have been shown to increase with normal aging (Braak and Braak, 1997). Even non-AD brain specimens from individuals as old as 90 years contain NFTs. In Braak stage I, NFTs are confined within the transentorhinal region. Most of these NFTs are not accompanied by SPs, suggesting that that NFT formation occurring within the transentorhinal region is independent of SP formation, and thus may not represent a pathological process linked to AD. In line with these data is the finding that the anatomical distribution of NFTs observed in Braak stage I appears to be age dependent (Braak and Braak, 1997), which is consistent with the premise that NFT development occurs as part of normal brain aging.

We detected an increased amount of granular tau oligomers in Braak-stage I frontal cortex samples but not in Braak-stage 0 samples, suggesting that, at a time when NFTs form in the entorhinal cortex, tau dysfunction, which tau comes up from microtubule, and forms aggregate, has already started to occur in the frontal cortex, which should indicate tau dysfunction (Lu and Wood, 1993; Yoshida and Ihara, 1993). Interestingly, the level of granular tau oligomers in frontal cortex remained constant in samples staged at Braak stages II–V, even though the density of NFTs increases progressively in these stages. At this point, however, we cannot explain the incongruity between the levels of tau oligomers and NFTs. We do not know exactly how granular tau oligomers affect neuronal vulnerability.

We also investigated the relationship between granular tau oligomer formation and the density and distribution of senile plaques (SPs) (data not shown), another neuropathological hallmark of AD. We found granular tau oligomers in samples containing SPs in the neocortex (SP-stage B and C). In one Braak-stage 0 sample from an SP-stage B patient (No. 6 in Table 1), however, we did not detect a significant increase in granular tau oligomer levels, suggesting that the extent of SP pathology may not affect the formation of granular tau oligomers. Recently, Katsuno and colleagues reported that the accumulation of AB and tau occurs independently in entorhinal cortex (Katsuno et al., 2005). Therefore, the formation of granular tau oligomers may not be related to Aβ accumulation but instead may be related to some other aging-related event that occurs during Braak stage I. In later Braak stages, Aβ may accelerate the formation of granular tau oligomers that ultimately leads to NFT formation and neuronal loss. Further studies are required in order to understand the precise biochemical sequence of events underlying neuronal death, NFT formation, and granular tau oligomer formation.

References

Braak, H., Braak, E., 1991. Neuropathological stageing of Alzheimer-related changes. Acta Neuropathol. (Berl) 239–259.

Braak, H., Braak, E., 1997. Frequency of stages of Alzheimer-related lesions in different age categories. Neurobiol. Aging 351–357.

Gomez-Isla, T., Hollister, R., West, H., Mui, S., Growdon, J.H., Petersen, R.C., Parisi, J.E., Hyman, B.T., 1997. Neuronal loss correlates with but exceeds neurofibrillary tangles in Alzheimer's disease. Ann. Neurol. 17–24.

Greenberg, S.G., Davies, P., 1990. A preparation of Alzheimer paired helical filaments that displays distinct tau proteins by polyacrylamide gel electrophoresis. Proc. Natl. Acad. Sci. U.S.A. 5827–5831.

Hansma, H.G., Laney, D.E., Bezanilla, M., Sinsheimer, R.L., Hansma, P.K., 1995. Applications for atomic force microscopy of DNA. Biophys. J. 1672–1677.

Ihara, Y., 2001. PHF and PHF-like fibrils—cause or consequence? Neurobiol. Aging 123–126.

Ihara, Y., Abraham, C., Selkoe, D.J., 1983. Antibodies to paired helical filaments in Alzheimer's disease do not recognize normal brain proteins. Nature 727–730.

Jicha, G.A., O'Donnell, A., Weaver, C., Angeletti, R., Davies, P., 1999. Hierarchical phosphorylation of recombinant tau by the paired-helical filament-associated protein kinase is dependent on cyclic AMP-dependent protein kinase. J. Neurochem. 214–224.

Katsuno, T., Morishima-Kawashima, M., Saito, Y., Yamanouchi, H., Ishiura, S., Murayama, S., Ihara, Y., 2005. Independent accumulations of tau and amyloid beta-protein in the human entorhinal cortex. Neurology 687–692.

Lee, V.M., Goedert, M., Trojanowski, J.Q., 2001. Neurodegenerative tauopathies. Annu. Rev. Neurosci. 1121–1159.

Lu, Q., Wood, J.G., 1993. Functional studies of Alzheimer's disease tau protein. J. Neurosci. 508–515.

Murayama, S., Saito, Y., 2004. Neuropathological diagnostic criteria for Alzheimer's disease. Neuropathology 254–260.

Reed, L.A., Wszolek, Z.K., Hutton, M., 2001. Phenotypic correlations in FTDP-17. Neurobiol. Aging 89–107.

Saito, Y., Ruberu, N.N., Sawabe, M., Arai, T., Tanaka, N., Kakuta, Y., Yamanouchi, H., Murayama, S., 2004. Staging of argyrophilic grains: an age-associated tauopathy. J. Neuropathol. Exp. Neurol. 911–918.

Santacruz, K., Lewis, J., Spires, T., Paulson, J., Kotilinek, L., Ingelsson, M., Guimaraes, A., DeTure, M., Ramsden, M., McGowan, E., Forster, C., Yue, M., Orne, J., Janus, C., Mariash, A., Kuskowski, M., Hyman, B., Hutton, M., Ashe, K.H., 2005. Tau suppression in a neurodegenerative mouse model improves memory function. Science 476–481.

Selkoe, D.J., Ihara, Y., Salazar, F.J., 1982. Alzheimer's disease: insolubility of partially purified paired helical filaments in sodium dodecyl sulfate and urea. Science 1243–1245.

Takashima, A., Murayama, M., Murayama, O., Kohno, T., Honda, T., Yasutake, K., Nihonmatsu, N., Mercken, M., Yamaguchi, H., Sugihara, S., Wolozin, B., 1998. Presenilin 1 associates with glycogen synthase kinase-3beta and its substrate tau. Proc. Natl. Acad. Sci. U.S.A. 9637–9641.

Tanemura, K., Akagi, T., Murayama, M., Kikuchi, N., Murayama, O., Hashikawa, T., Yoshiike, Y., Park, J.M., Matsuda, K., Nakao, S., Sun, X., Sato, S., Yamaguchi, H., Takashima, A., 2001. Formation of filamentous tau aggregations in transgenic mice expressing V337M human tau. Neurobiol. Dis. 1036–1045.

Tanemura, K., Murayama, M., Akagi, T., Hashikawa, T., Tominaga, T., Ichikawa, M., Yamaguchi, H., Takashima, A., 2002. Neurodegeneration with tau accumulation in a transgenic mouse expressing V337M human tau. J. Neurosci. 133–141.

Tatebayashi, Y., Miyasaka, T., Chui, D.H., Akagi, T., Mishima, K., Iwasaki, K., Fujiwara, M., Tanemura, K., Murayama, M., Ishiguro, K., Planel, E., Sato, S., Hashikawa, T., Takashima, A., 2002. Tau filament formation and associative memory deficit in aged mice expressing mutant (R406W) human tau. Proc. Natl. Acad. Sci. U.S.A. 13896–13901.

von Bergen, M., Barghorn, S., Biernat, J., Mandelkow, E.M., Mandelkow, E., 2005. Tau aggregation is driven by a transition from random coil to beta sheet structure. Biochim. Biophys. Acta 158–166.

Wittmann, C.W., Wszolek, M.F., Shulman, J.M., Salvaterra, P.M., Lewis, J., Hutton, M., Feany, M.B., 2001. Tauopathy in *Drosophila*: neurodegeneration without neurofibrillary tangles. Science 711–714.

Yoshida, H., Ihara, Y., 1993. Tau in paired helical filaments is functionally distinct from fetal tau: assembly incompetence of paired helical filament-tau. J. Neurochem. 1183–1186.